Supporting Information for

Tuning Central Fused Ring and Terminal Units to Improve Photovoltaic Performance for the Ar(A-D)$_2$ Type Small Molecules in Solution-Processed Organic Solar Cells

Jianhua Chen,[a,1] Linrui Duan,[a,1] Manjun Xiao, [a] Qiong Wang, [a] Bin Liu, [a] Hao Xia,[a] Renqiang Yang,[*,b] Weiguo Zhu[*,a,b]

Contents

1. Experiment part.

1.1 Synthesis of **DPP_2Py**

Compound $Py(BPin)_2$ (45.4 mg, 0.1 mmol), compound DPP-Br (132.9 mg, 0.22 mmol), 2.0 M K_2CO_3 aqueous solution (1.0 mL), methanol (1.0 mL), and toluene (5.0 mL) were mixed together in a 25 mL two-neck flask and purged with nitrogen flow for 20 min. To this solution was added tetrakis(triphenylphosphine)palladium (10 mg). The reaction mixture was heated to 80 °C and refluxed for 12 h. Then allowed mixture to cool to room temperature and extracted with CH_2Cl_2 (25 mL × 3). The resulting organic layer was washed with brine, dried over anhydrous $MgSO_4$ and evaporated to remove off solvent under vacuum. The residue was purified by column chromatography on silica gel using CH_2Cl_2/petroleum ether (2:1, *v/v*) as eluent to provide a dark blue powder (106.4 mg, 85.3%). ^{1}H NMR ($CDCl_3$, 400 MHz), δ (ppm): 8.95 (d, J = 2.8 Hz, 2H), 8.89 (s, 2H), 8.19 (s, 4H), 8.00 (s, 4H), 7.59 (d, J = 2.4 Hz, 2H), 7.54 (d, J = 4.2 Hz, 2H), 7.21 (s, 2H), 4.05 (d, J = 31.7 Hz, 8H), 1.91 (d, J = 26.7 Hz, 4H), 1.52-1.12 (m, 32H), 1.03-0.76 (m, 24H). MALDI-MS (m/z) of $C_{76}H_{86}N_4O_4S_4$ for [M^+]: calcd. 1247.78; found, 1247.80. Elemental analysis for $C_{76}H_{86}N_4O_4S_4$: calcd. C, 73.15; H, 6.95; N, 4.49; found C, 73.09; H, 7.98; N, 4.46.

1.2 Synthesis of **DPP-Th**

Under the protection of argon, to a solution of DPP-Br (1.21 g, 2 mmol) and Th-Sn (1.07 g, 2.2 mmol) in 50 mL toluene was added tetrakis(triphenylphosphine) palladium (115.6 mg, 0.1 mmol). The reaction mixture was heated to 110 °C and refluxed for 16 h. Then allowed mixture to cool to room temperature and extracted with CH_2Cl_2 (50 mL × 3). The resulting organic layer was washed with brine, dried over anhydrous $MgSO_4$ and evaporated to remove off solvent under vacuum. The residue was purified by column chromatography on silica gel using CH_2Cl_2/petroleum ether (1:1, *v/v*) as eluent to provide a purple powder (1.21 g, 84.6%). ^{1}H NMR (400 MHz, $CDCl_3$) δ 8.88 (d, J = 4.1 Hz, 1H), 8.80 (d, J = 3.5 Hz, 1H), 7.55 (d, J = 4.8 Hz,

1H), 7.21 (d, *J* = 4.8 Hz, 1H), 7.18 (d, *J* = 4.8 Hz, 1H), 7.18 (d, *J* = 4.1 Hz, 1H), 7.08 (d, *J* = 3.5 Hz, 1H), 6.68 (d, *J* = 3.4 Hz, 1H), 4.07 – 3.87 (m, 4H), 2.76 (t, *J* = 7.5 Hz, 2H), 1.91 – 1.72 (m, 2H), 1.63 (dd, *J* = 14.6, 7.3 Hz, 2H), 1.41 – 1.08 (m, 26H), 0.90 – 0.71 (m, 15H). ^{13}C NMR (101 MHz, $CDCl_3$) δ 161.86, 161.59, 147.88, 143.69,140.34, 139.53, 137.04, 134.98, 133.60, 130.20, 130.01, 128.39, 127.38, 125.38, 125.07, 124.03, 108.25, 107.87, 45.94, 39.27, 39.13, 31.87, 31.56, 30.39, 30.31, 30.27, 29.72, 29.32, 29.21, 29.09, 28.58, 28.40, 23.73, 23.61, 23.13, 23.08, 22.67, 14.10, 14.07, 14.02, 10.58, 10.54. MALDI-MS (m/z) of $C_{42}H_{58}N_2O_2S_3$ for [M^+]: calcd. 718.37; found, 718.49.

1.3 Synthesis of **DPP-Th-Br**

At 0 °C, to a solution of **DPP-Th** (1.21 g, 1.68 mmol) in 100 mL chloroform was added N-Bromosuccinimide (0.36 g, 2.02 mmol). The reaction mixture was stirred at this temperature for 4 h, and then poured into 200 mL water. Then extracted with CH_2Cl_2 (50 mL × 3). The resulting organic layer was washed with brine, dried over anhydrous $MgSO_4$ and evaporated to remove off solvent under vacuum. The residue was purified by column chromatography on silica gel using CH_2Cl_2/petroleum ether (1:1, *v/v*) as eluent to provide a blue powder (1.25 g, 93.3%). ^{1}H NMR (400 MHz, $CDCl_3$) δ 8.90 (d, *J* = 4.1 Hz, 1H), 8.53 (d, *J* = 4.1 Hz, 1H), 7.17 (d, *J* = 4.1 Hz, 1H), 7.15 (d, *J* = 4.2 Hz, 1H), 7.09 (d, *J* = 3.5 Hz, 1H), 6.68 (d, *J* = 3.4 Hz, 1H), 4.03 – 3.93 (m, 2H), 3.89 (t, *J* = 6.8 Hz, 2H), 2.76 (t, *J* = 7.5 Hz, 2H), 1.82 (d, *J* = 27.1 Hz, 2H), 1.70 – 1.56 (m, 2H), 1.40 – 1.12 (m, 26H), 0.84 (m, 15H). ^{13}C NMR (101 MHz, $CDCl_3$) δ 161.75, 161.30, 148.06 , 144.06, 140.78, 137.99, 137.37, 136.69, 134.77 , 131.45, 131.35, 127.25, 125.42, 125.17, 124.06, 118.24, 108.46, 107.70, 46.01, 39.25, 39.16, 31.87, 31.55, 30.39, 30.33, 30.25, 29.32, 29.21, 29.10, 28.57, 28.39, 28.38, 23.72, 23.64, 23.12, 23.06, 22.67, 14.10, 14.07, 14.02, 10.57, 10.53. MALDI-MS (m/z) of $C_{42}H_{57}BrN_2O_2S_3$ for [M^+]: calcd. 798.27; found, 798.42.

1.4 Synthesis of **ThDPP2-Py**

Compound $Py(BPin)_2$ (45.4 mg, 0.1 mmol), compound **DPP-Th-Br** (175.6 mg, 0.22 mmol), 2.0 M K_2CO_3 aqueous solution (1.0 mL), methanol (1.0 mL), and toluene (5.0 mL) were mixed together in a 25 mL two-neck flask and purged with nitrogen flow

for 20 min. To this solution was added tetrakis(triphenylphosphine)palladium (10 mg). The reaction mixture was heated to 80 °C and refluxed for 12 h. Then allowed mixture to cool to room temperature and extracted with CH_2Cl_2 (25 mL × 3). The resulting organic layer was washed with brine, dried over anhydrous $MgSO_4$ and evaporated to remove off solvent under vacuum. The residue was purified by column chromatography on silica gel using CH_2Cl_2/petroleum ether (2:1, *v/v*) as eluent to provide a dark blue powder (113.4 mg, 69.3%). ^{1}H NMR (400 MHz, $CDCl_3$) δ 8.92 (s, 4H), 7.98 (s, 4H), 7.91 (s, 4H), 7.44 (s, 2H), 7.07 (s, 2H), 6.99 (s, 2H), 6.60 (s, 2H), 3.96 (d, *J* = 17.9 Hz, 8H), 2.69 (d, *J* = 6.9 Hz, 4H), 1.91 (s, 4H), 1.61 - 1.0 (m, 56H), 1.08 – 0.80 (m, 30H). MALDI-MS (m/z) of $C_{100}H_{122}N_4O_4S_6$ for [M^+]: calcd. 1635.78; found, 1636.64.

1.5 Synthesis of **TPADPP2-Py**

Compound $Py(BPin)_2$ (45.4 mg, 0.1 mmol), compound **TPADPP-Br** (242.8 mg, 0.22 mmol), 2.0 M K_2CO_3 aqueous solution (1.0 mL), methanol (1.0 mL), and toluene (5.0 mL) were mixed together in a 25 mL two-neck flask and purged with nitrogen flow for 20 min. To this solution was added tetrakis(triphenylphosphine)palladium (10 mg). The reaction mixture was heated to 80 °C and refluxed for 12 h. Then allowed mixture to cool to room temperature and extracted with CH_2Cl_2 (25 mL × 3). The resulting organic layer was washed with brine, dried over anhydrous $MgSO_4$ and evaporated to remove off solvent under vacuum. The residue was purified by column chromatography on silica gel using CH_2Cl_2/petroleum ether (2:1, *v/v*) as eluent to provide a dark blue powder (180.5 mg, 80.4%). ^{1}H NMR (400 MHz, $CDCl_3$) δ 9.02 (d, *J* = 3.3 Hz, 2H), 8.94 (s, 2H), 8.03 (s, 4H), 7.95 (s, 4H), 7.48 (s, 2H), 7.34 (s, 2H), 7.33 (s, 2H), 7.19 (s, 2H), 7.00 (s, 4H), 6.97 (s,4H), 6.81 (s, 6H), 6.79 (s, 6H), 3.93 (m, 16H), 1.94 (s, 4H), 1.85 – 1.71 (m, 8H), 1.54 – 1.20 (m, 72H), 1.06 – 0.80 (m, 36H). MALDI-MS (m/z) of $C_{144}H_{176}N_6O_8S_4$ for [M^+]: calcd. 2246.25; found, 2246.60.

2. TGA curves of DPP_2Py, $ThDPP_2Py$ and $TPADPP_2Py$.

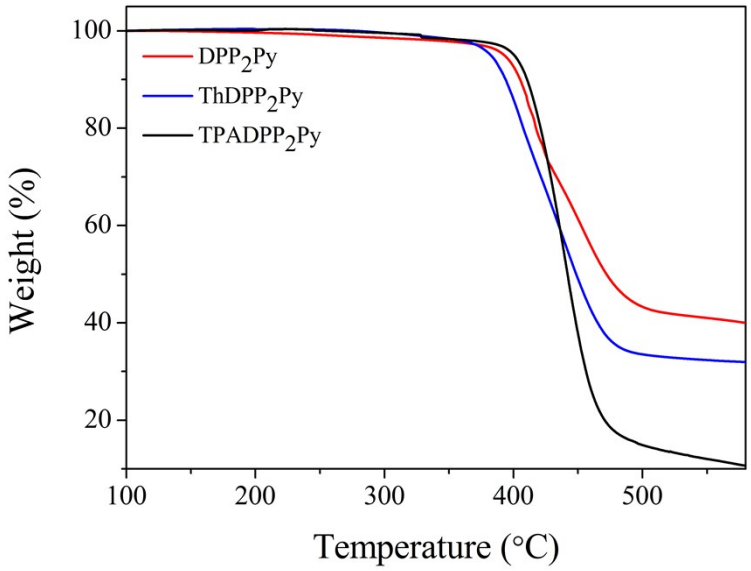

Fig. S1. The TGA curves of DPP_2Py, $ThDPP_2Py$ and $TPADPP_2Py$.

3. Photovoltaic properties of the $DPP_2Py/PC_{71}BM$-based OPV cells

D/A ratio	DIO ratio	Annealed temperature (℃)	V_{OC} (V)	J_{SC} (mA/cm^2)	*FF* (%)	PCE$_{max}$ (%)
1 : 1	0%	25	0.85	6.63	54.31	3.05
1 : 1	1%	25	0.83	10.57	54.35	4.76
1 : 1	2%	25	0.82	9.29	58.08	4.43
1.5 : 1	1%	25	0.84	9.89	50.85	4.23
2 : 1	1%	25	0.82	9.29	58.08	4.43
1 : 1	1%	80	0.85	11.14	57.42	4.96
1 : 1	1%	110	0.85	11.13	60.07	5.67
1 : 1	1%	140	0.82	10.74	45.54	4.02
1 : 1	0%	110	0.86	8.30	50.49	3.59
1 : 1	0.5%	110	0.85	8.79	51.55	3.86
1 : 1	1.5%	110	0.84	11.86	53.64	5.32
1 : 1	2%	110	0.83	11.85	51.09	5.08

Table S1. Photovoltaic performance of the DPP_2Py-based OPV cells.

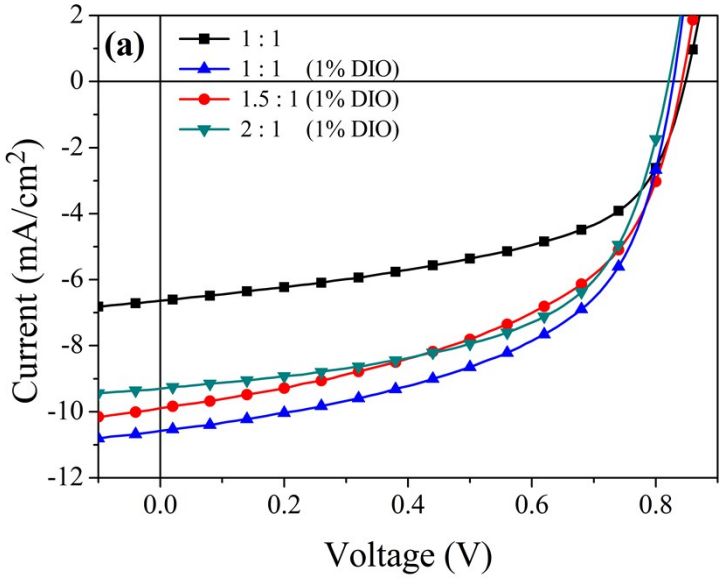
(a)
1 : 1
1 : 1 (1% DIO)
1.5 : 1 (1% DIO)
2 : 1 (1% DIO)
Current (mA/cm2)
Voltage (V)

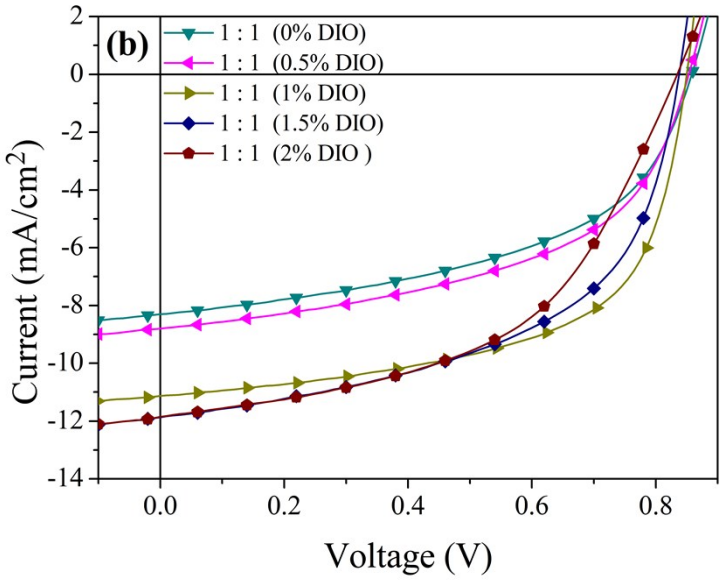
(b)
1 : 1 (0% DIO)
1 : 1 (0.5% DIO)
1 : 1 (1% DIO)
1 : 1 (1.5% DIO)
1 : 1 (2% DIO)
Current (mA/cm2)
Voltage (V)

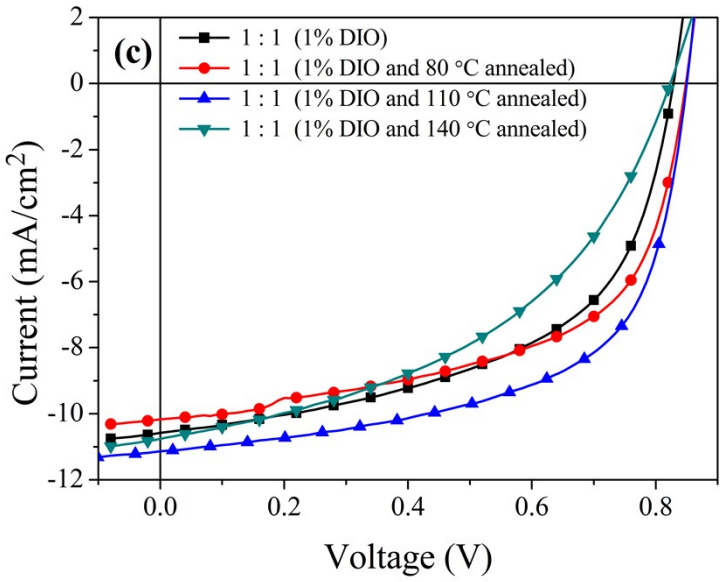

Fig. S2. *J-V* characteristics of the $DPP_2Py/PC_{71}BM$ based OPV cells under AM.1.5G illumination (100 mW/cm^2). (a) D/A ratio optimization; (b) DIO optimization; (c) annealing temperature optimization. The optimized condition is D/A ratio of 1:1 with 1% DIO and annealed at 110 ˚C for 10 minutes.

4. Photovoltaic properties of the $ThDPP_2Py/PC_{71}BM$-based OPVcells

D/A ratio	DIO ratio	Annealed temperature (ºC)	V_{OC} (V)	J_{SC} (mA/cm^2)	*FF* (%)	PCE*max*/*ave*[a] (%)
1 : 1	0%	25	0.66	3.15	56.54	1.17
1 : 1	0.5%	25	0.67	12.54	62.41	5.27
1 : 1	1%	25	0.66	15.35	57.89	5.88
1 : 1	1.5%	25	0.66	12.61	54.94	4.57
1.2 : 1	1%	25	0.66	13.04	56.92	4.89
1.5 : 1	1%	25	0.66	12.66	57.55	4.70
2 : 1	1%	25	0.66	8.00	49.70	2.86
1 : 2	1%	25	0.66	13.34	61.25	5.38
1 : 1	1%	110	0.67	12.68	54.65	4.63

Table S2. Photovoltaic performance of the $ThDPP_2Py$-based OPV cells.

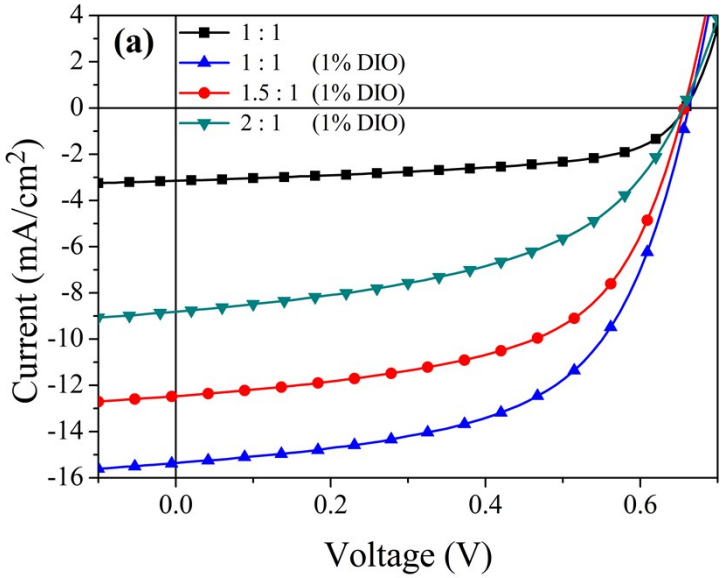
(a)
1 : 1
1 : 1 (1% DIO)
1.5 : 1 (1% DIO)
2 : 1 (1% DIO)
Current (mA/cm2)
Voltage (V)

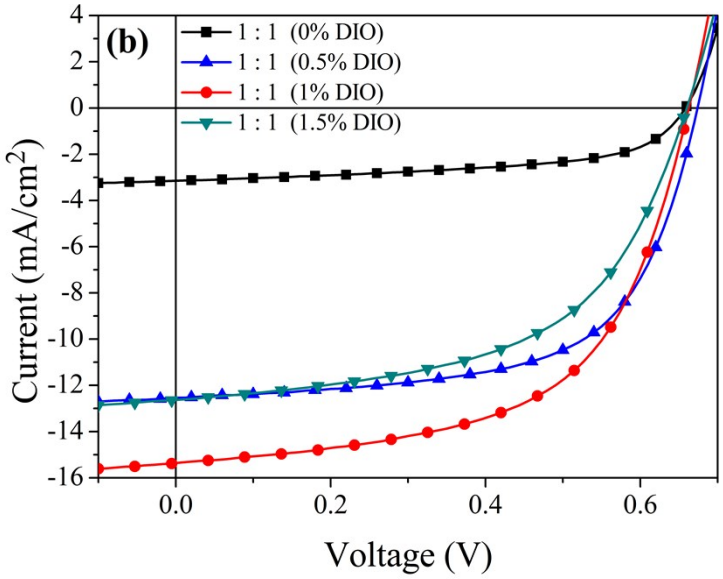
(b)
1 : 1 (0% DIO)
1 : 1 (0.5% DIO)
1 : 1 (1% DIO)
1 : 1 (1.5% DIO)
Current (mA/cm2)
Voltage (V)

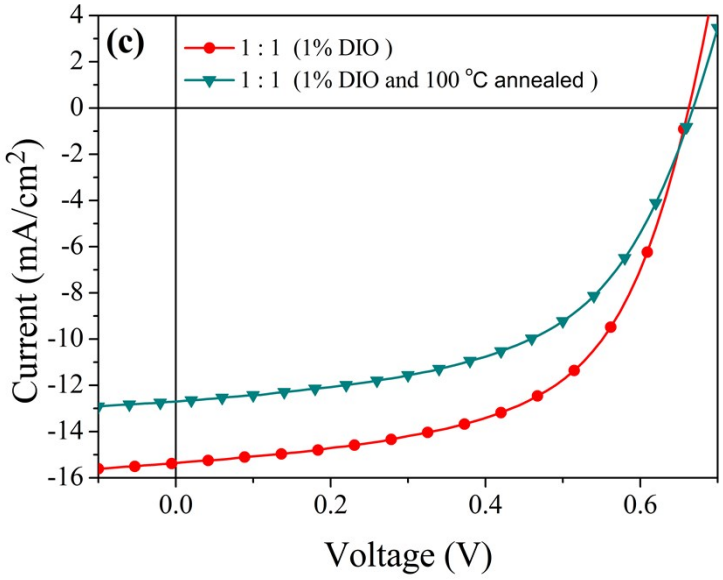

Fig. S3. *J-V* characteristics of the ThDPP$_2$Py/PC$_{71}$BM based OPV cells under AM.1.5G illumination (100 mW/cm^2): (a) D/A ratio optimization; (b) DIO optimization; (c) annealing temperature optimization. The optimized condition is D/A ratio of 1:1 with 1% DIO without annealing.

5. Photovoltaic properties of the TPADPP$_2$Py/PC$_{71}$BM-based OPV cells

D/A ratio	DIO ratio	Annealed temperature (ºC)	V_{OC} (V)	J_{SC} (mA/cm^2)	*FF* (%)	PCE*max*/*ave*[a] (%)
1 : 1	0%	25	0.62	2.08	53.35	0.68
1 : 1	0.5%	25	0.62	8.12	56.83	2.87
1 : 1	1%	25	0.62	10.77	63.94	4.26
1 : 1	1.5%	25	0.63	10.74	56.56	3.82
1.5 : 1	1%	25	0.61	10.82	62.70	4.15
2 : 1	1%	25	0.62	7.68	53.46	2.55
1 : 1	1%	110	0.61	8.10	52.53	2.62

Table S3. Photovoltaic performance of the TPADPP$_2$Py-based OPV cells.

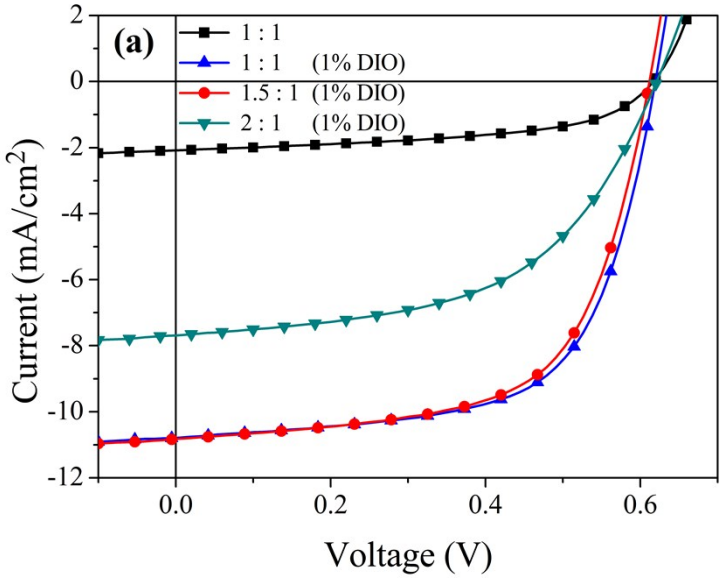
(a)
1 : 1
1 : 1 (1% DIO)
1.5 : 1 (1% DIO)
2 : 1 (1% DIO)
Current (mA/cm2)
Voltage (V)
2
0
-2
-4
-6
-8
-10
-12
0.0
0.2
0.4
0.6

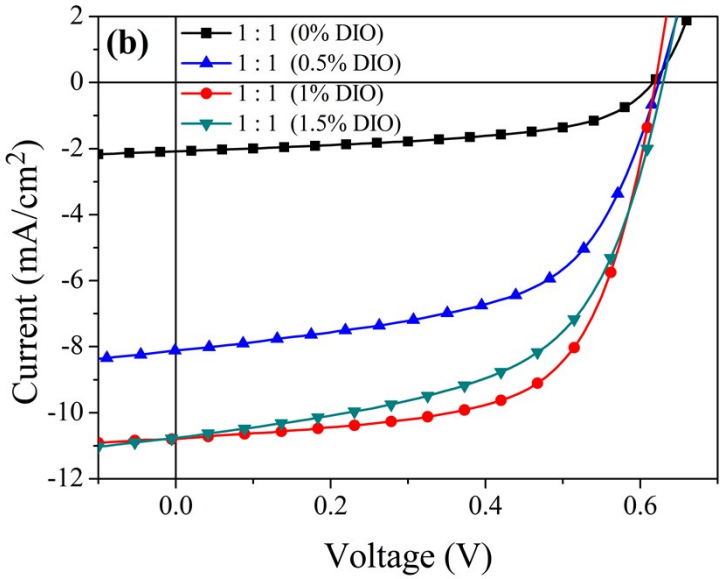
(b)
1 : 1 (0% DIO)
1 : 1 (0.5% DIO)
1 : 1 (1% DIO)
1 : 1 (1.5% DIO)
Current (mA/cm2)
Voltage (V)
2
0
-2
-4
-6
-8
-10
-12
0.0
0.2
0.4
0.6

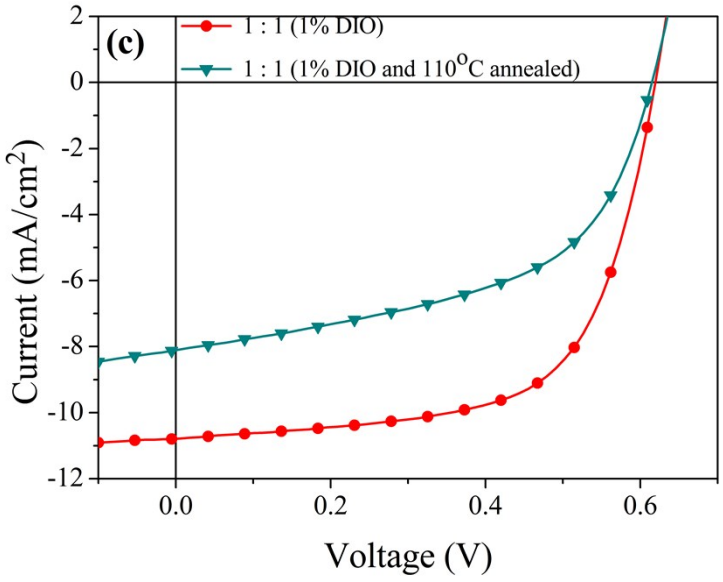

Fig. S4. *J-V* characteristics of the TPADPP$_2$Py/PC$_{71}$BM based OPV cells under AM.1.5G illumination (100 mW/cm^2): (a) D/A ratio optimization; (b) DIO optimization; (c) annealing temperature optimization. The optimized condition is D/A ratio of 1:1 with 1% DIO without annealing.

6. The comparison of the photovoltaic performance of DPP$_2$Py and other reported DPP$_2$Ar analogies.

Table S4. The comparison of photovoltaic performance of DPP$_2$Py/PC$_{71}$BM and other DPP$_2$Ar/PC$_{71}$BM based OPV cells.

SMs	V_{OC} (V)	J_{SC} (mA/cm^2)	*FF* (%)	PCE $_{max}$(%)	μ_h(cm^2/Vs)	Reference
DPP$_2$Py[a,c]	0.85	11.13	60.07	5.67	8.47×10^{-4}	This work
DPP$_2$An[a]	0.82	11.90	55.40	5.44	4.02×10^{-4}	Our previous work[1]
DPP$_2$Na[b]	0.87	9.5	53	4.4	1.1×10^{-3}	Jo's work[2]
DPP$_2$Ph[d]	0.93	9.09	47	4.01	8.8×10^{-5}	Jo's work[3]
DPP$_2$[d]	0.84	7.40	37	2.31	6.0×10^{-5}	Jo's work[3]

[a]1% DIO; [b]0.5% DIO; [c] annealed at 110 °C; [d]annealed at 120 °C.

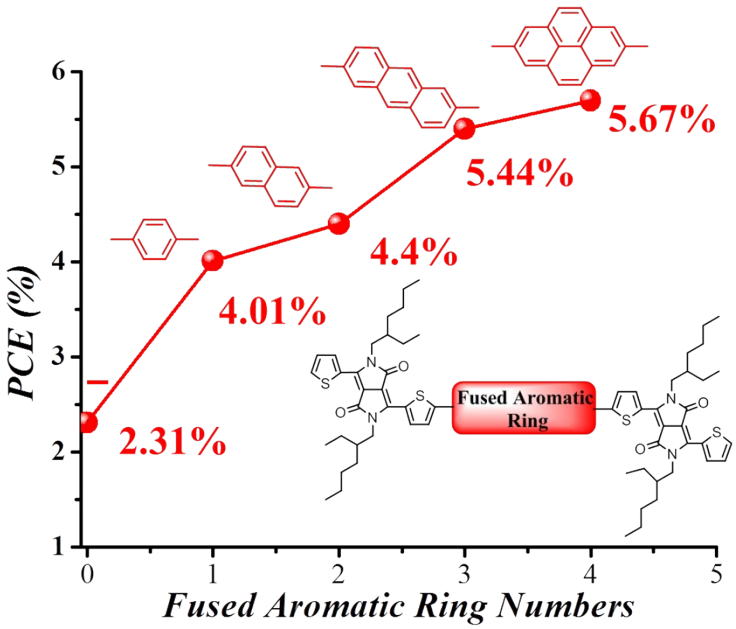

Fig. S5. Graphical comparison of $DPP_2Py/PC_{71}BM$ and other $DPP_2Ar/PC_{71}BM$ based OPV cells

7. The film morphologies of SMs/PC_{71}BM-based OPV cells under optimized conditions.

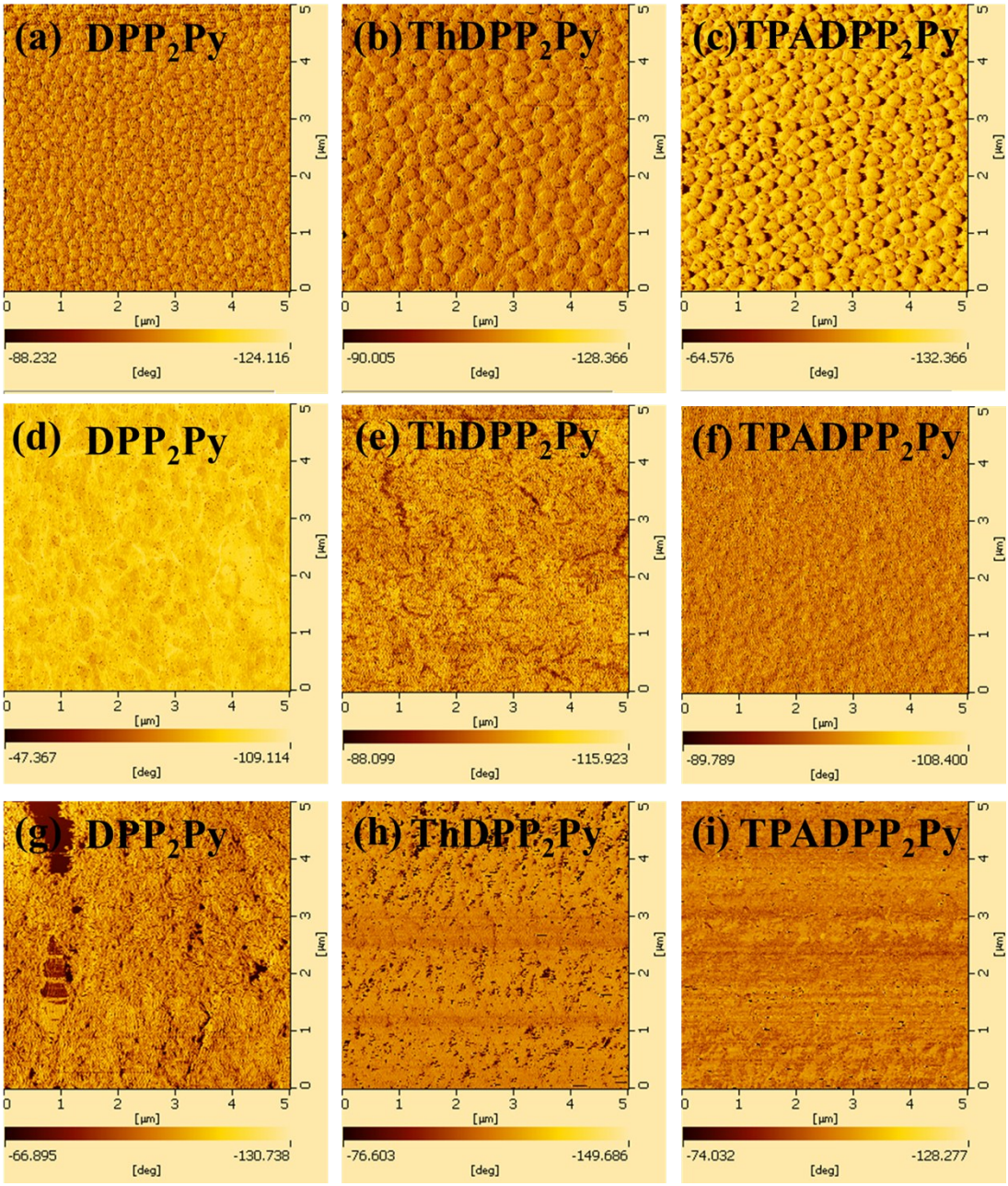

Fig. S6. AFM phase images (5×5 µm) of the SMs/$PC_{71}BM$ (1:1) blend films (a-c); SMs/$PC_{71}BM$ (1:1) with 1% DIO (d-e); SMs/$PC_{71}BM$ (1:1) with 1% DIO and annealed at 110 °C for 10 minutes (g-i); respectively.

8. NMR and MS spectra of SMs

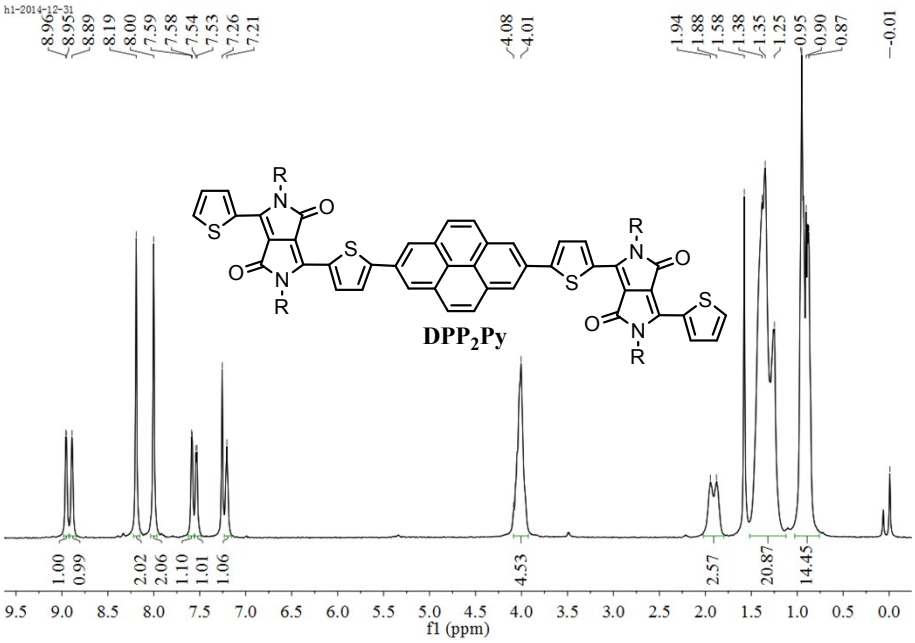

Fig. S7. ^{1}H NMR spectrum of DPP$_2$P***y***.

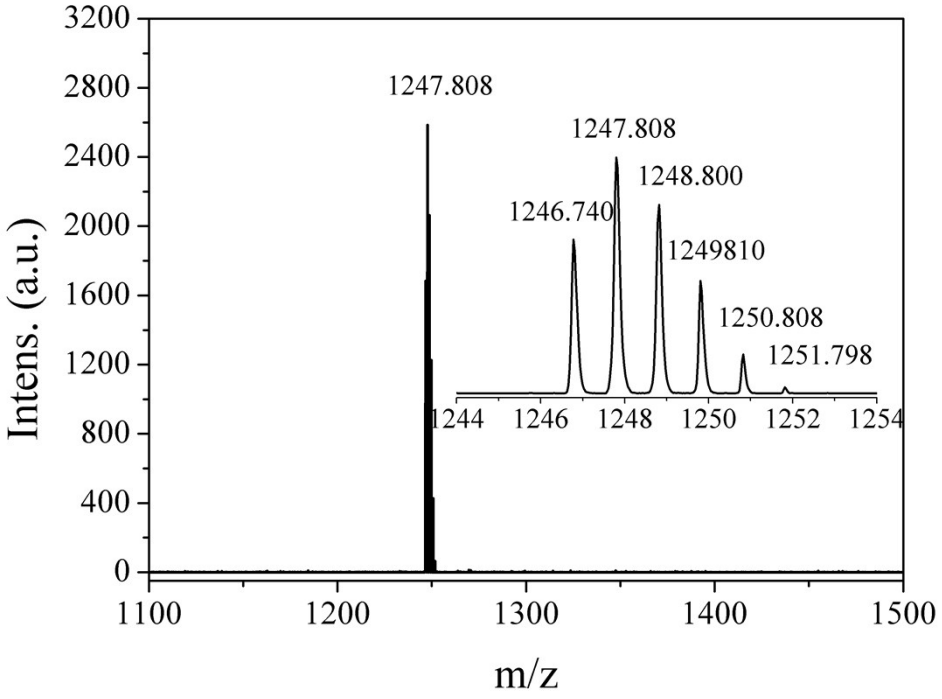

Fig. S8. TOF-MS spectra of DPP$_2$Py**.**

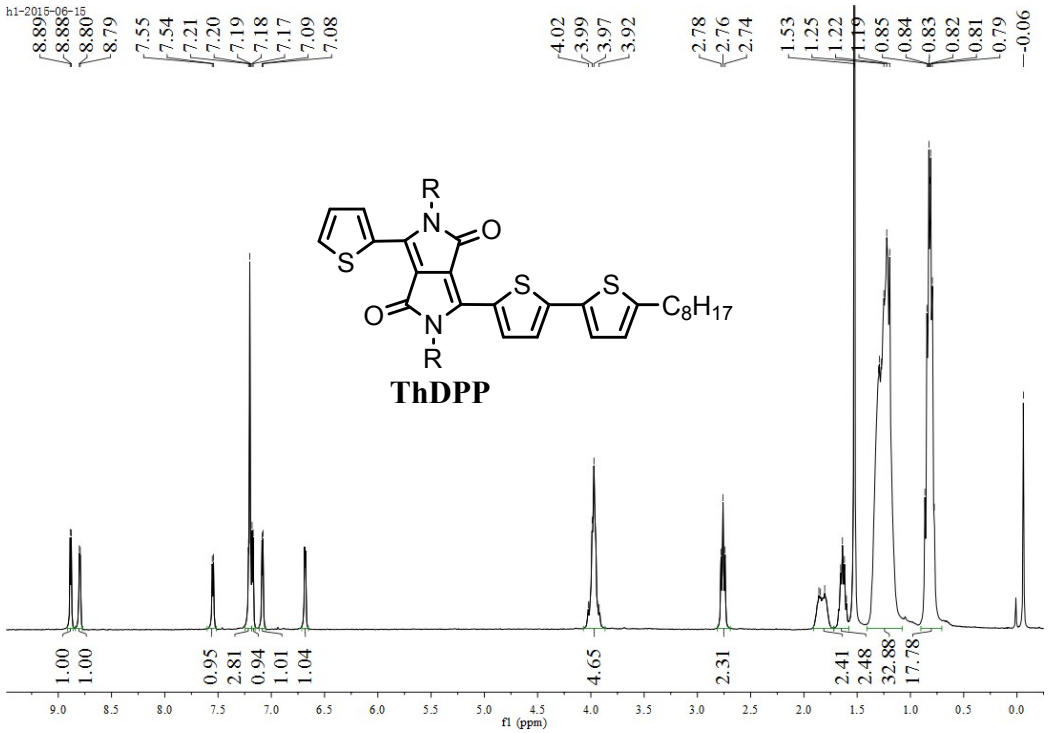

Fig. S9. ^{1}H NMR spectrum of ThDPP.

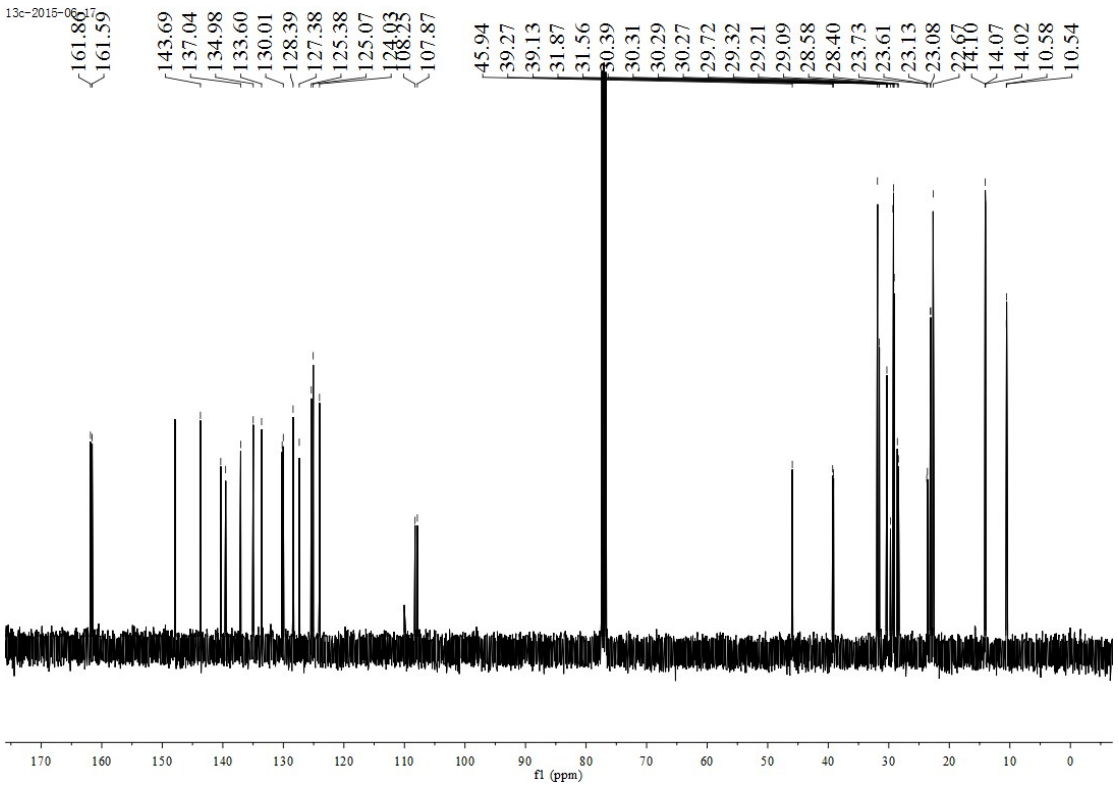

Fig. S10. ^{13}C NMR spectrum of ThDPP.

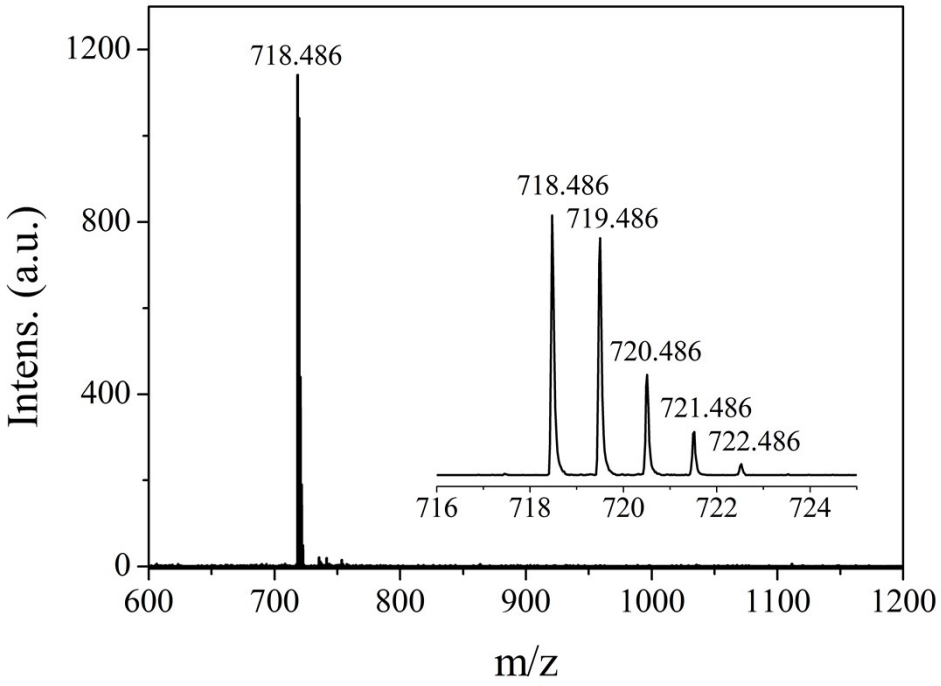

Fig. S11. TOF-MS spectra of ThDPP.

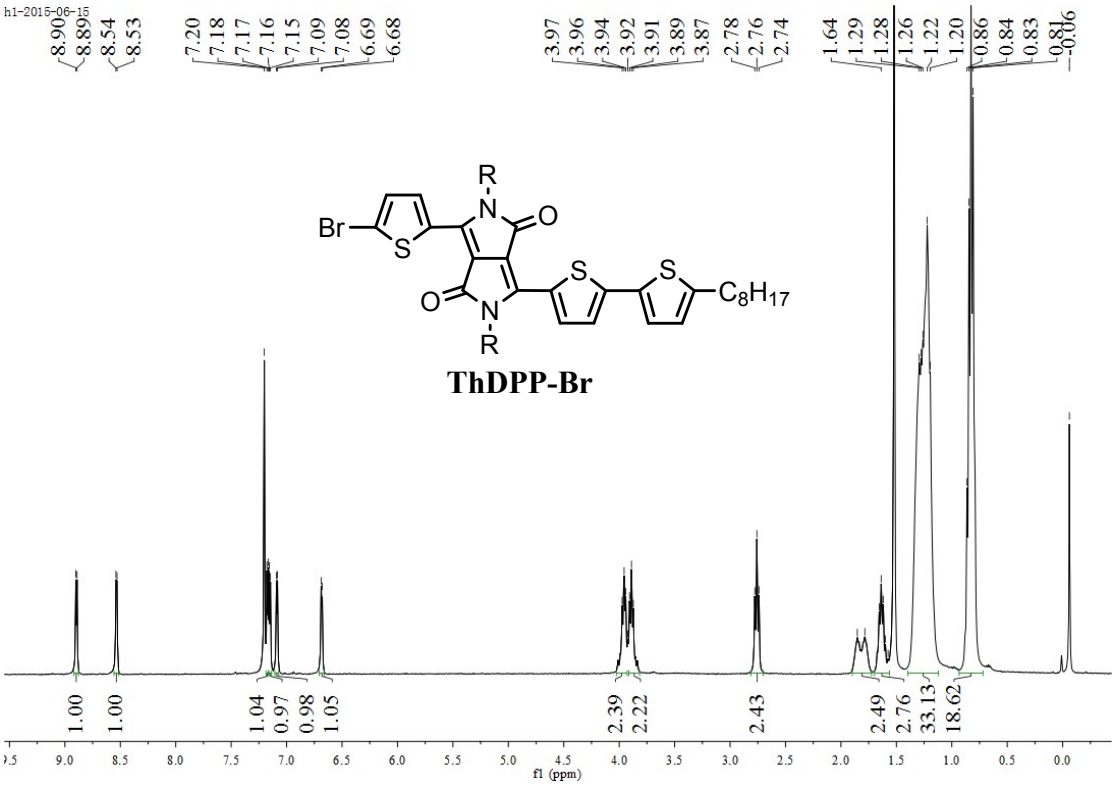

Fig. S12. ^{1}H NMR spectrum of of ThDPP-Br.

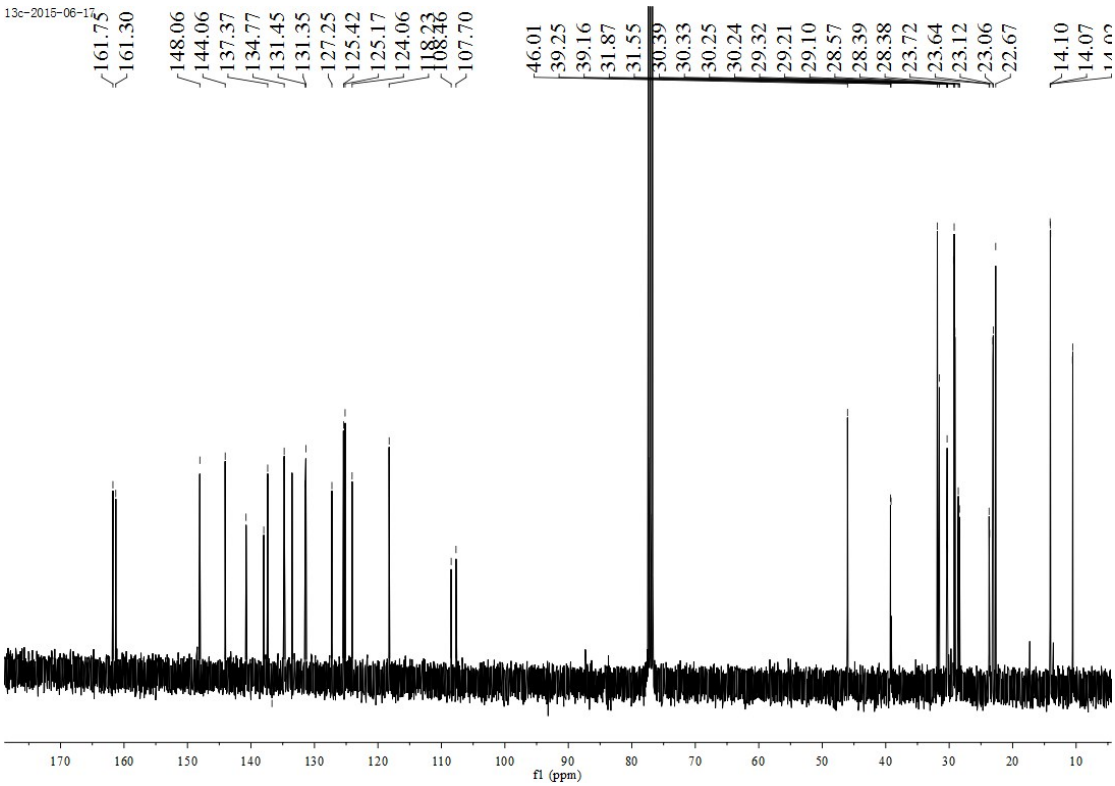

Fig. S13. ^{13}C NMR spectrum of ThDPP-Br.

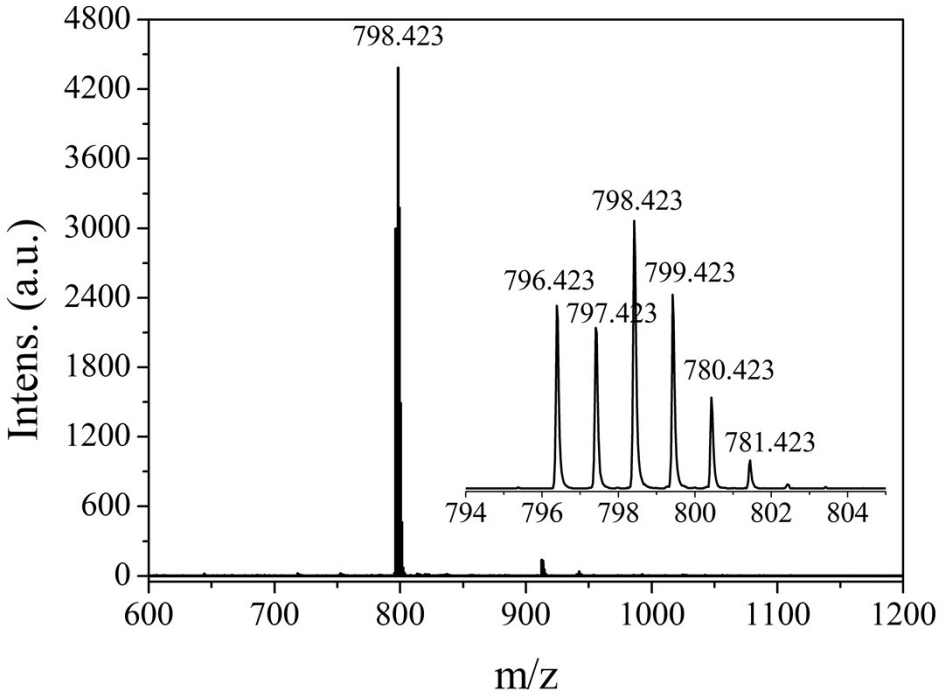

Fig. S14. TOF-MS spectra of ThDPP-Br.

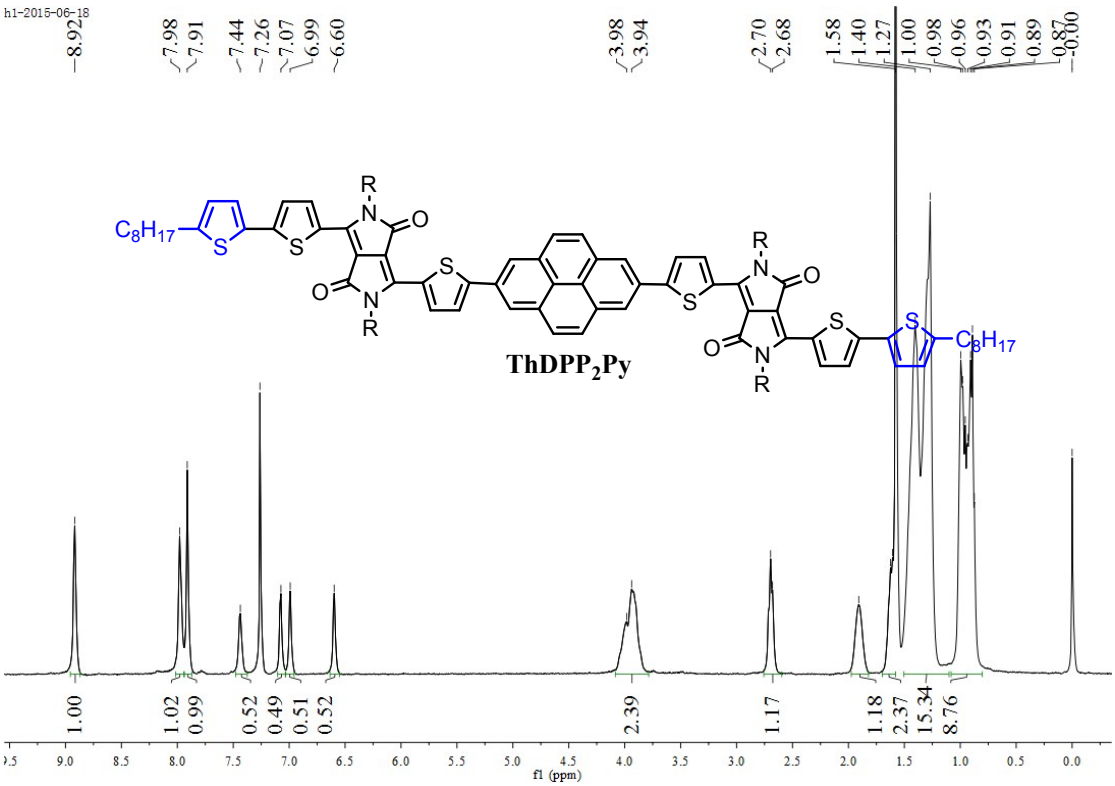

Fig. S15. ^{1}H NMR spectrum of of ThDPP$_2$Py.

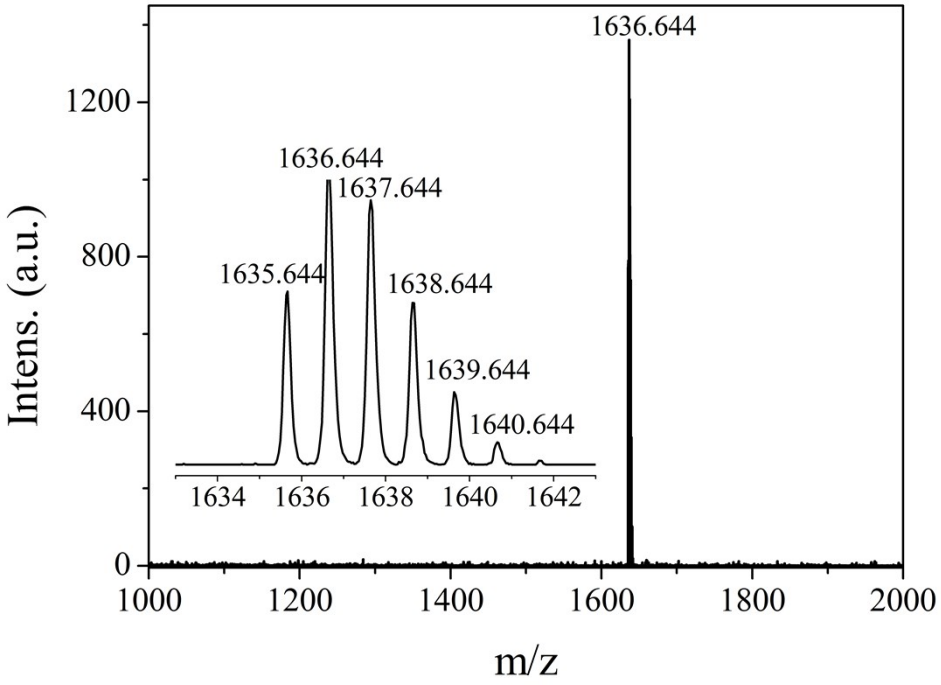

Fig. S16. TOF-MS spectra of ThDPP$_2$Py.

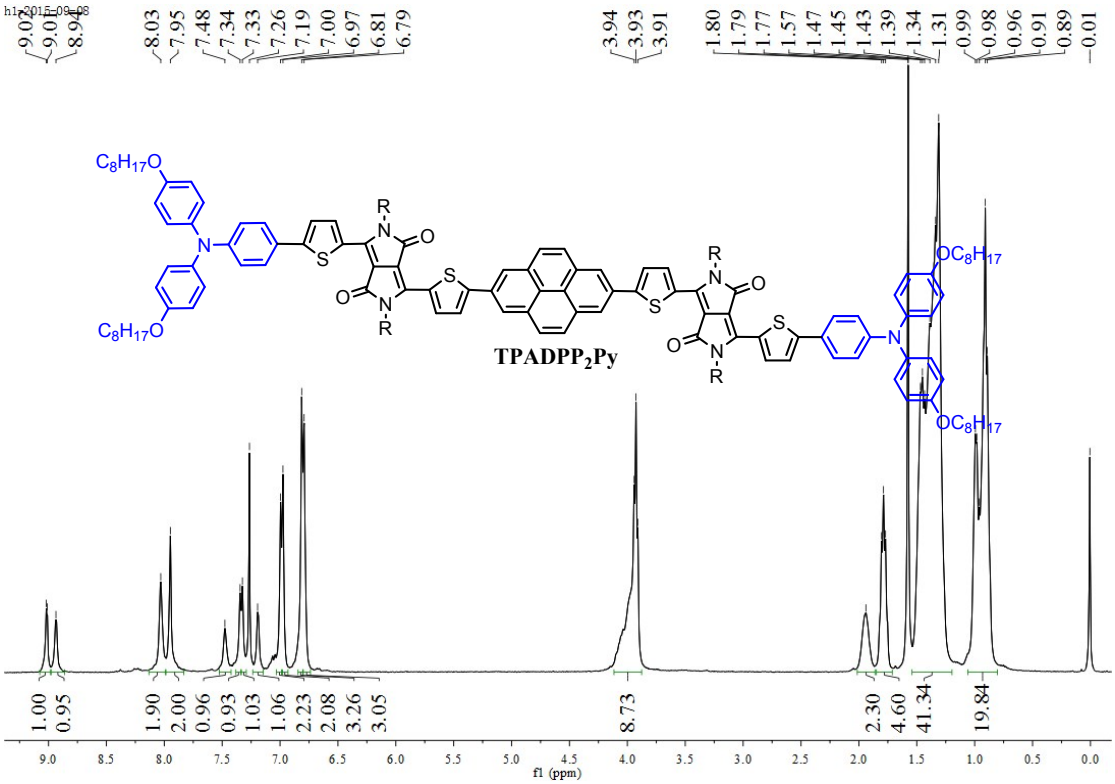

Fig. S17. ^{1}H NMR spectrum of of TPADPP$_2$Py.

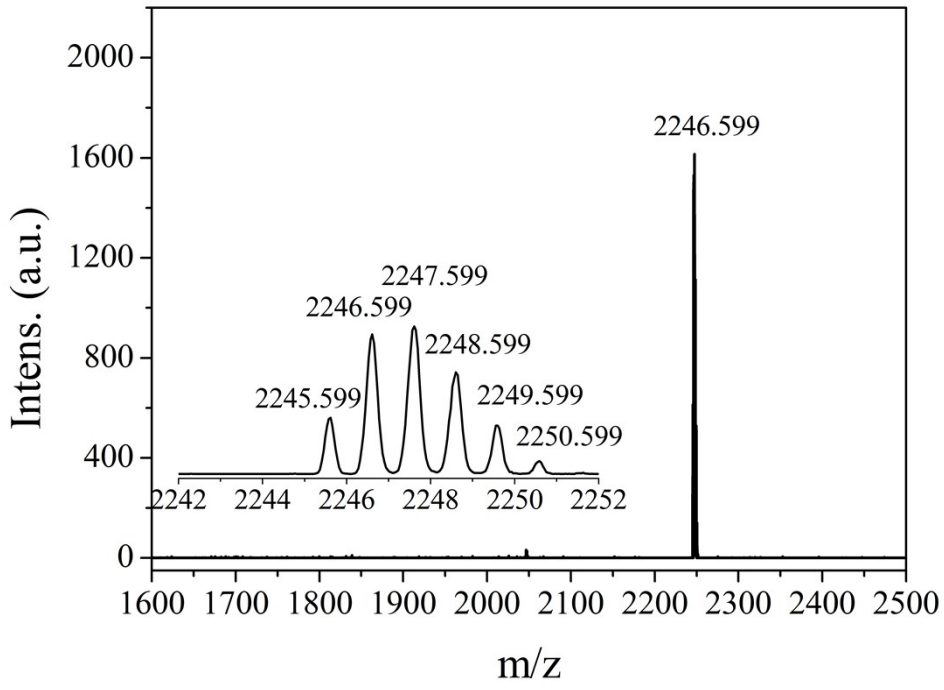

Fig. S18. TOF-MS spectra of TPADPP$_2$Py.

Reference:

1. X. Duan, M. Xiao, J. Chen, X. Wang, W. Peng, L. Duan, H. Tan, G. Lei, R. Yang, W. Zhu, *ACS Appl. Mater. Interface*s, 2015, **7**, 18292−18299.
2. J. W. Lee, Y. S. Choi and W. H. Jo, *Org. Electronics*, 2012, **13**, 3060-3066;
3. Y. S. Choi and W. H. Jo, *Org. Electronics*, 2013, **14**, 1621-1628.